Parkinsonism and Related Disorders 19 (2013) 47–52

Contents lists available at SciVerse ScienceDirect

Parkinsonism and Related Disorders

journal homepage: www.elsevier.com/locate/parkreldis

In vivo microglia activation in very early dementia with Lewy bodies, comparison with Parkinson's disease

S. Iannaccone [a], C. Cerami [a,b,c], M. Alessio [d], V. Garibotto [b], A. Panzacchi [b], S. Olivieri [d], G. Gelsomino [b], R.M. Moresco [b,e,f], D. Perani [b,c,e,*]

[a] *Neurorehabilitation Unit, Department of Clinical Neurosciences, San Raffaele Scientific Institute and Vita-Salute University, Milan, Italy*
[b] *Nuclear Medicine Unit and Division of Neuroscience, San Raffaele Scientific Institute, Milan, Italy*
[c] *Vita-Salute San Raffaele University, Milan, Italy*
[d] *Proteome Biochemistry Unit, San Raffaele Scientific Institute, Milan, Italy*
[e] *IBFM-CNR, Segrate, Italy*
[f] *University of Milano-Bicocca, Monza, Italy*

ARTICLE INFO

Article history:
Received 27 February 2012
Received in revised form
1 May 2012
Accepted 1 July 2012

Keywords:
[^{11}C]-PK11195
PET
Lewy bodies dementia
Early Parkinson disease
Microglia activation

ABSTRACT

Background: Reactive microgliosis, hallmark of neuroinflammation, may contribute to neuronal degeneration, as shown in several neurodegenerative diseases. We *in vivo* evaluated microglia activation in early dementia with Lewy bodies, still not reported, and compared with early Parkinson's disease, to assess possible differential pathological patterns.
Methods: We measured the [^{11}C]-PK11195 binding potentials with Positron Emission Tomography, using a simplified reference tissue model, as marker of microglia activation, and cerebral spinal fluid protein carbonylation levels, as marker of oxidative stress. Six dementia with Lewy bodies and 6 Parkinson's disease patients within a year from the onset, and eleven healthy controls were included. Clinical diagnosis was confirmed at a 4-year follow-up.
Results: In dementia with Lewy bodies as well as in Parkinson's disease, we found significant ($p < 0.001$) [^{11}C]-PK11195 binding potential increases in the substantia nigra and putamen. Patients with Lewy bodies dementia had extensive additional microglia activation in several associative cortices. This was evident also at a single subject level. Significant increase of Cerebral Spinal Fluid protein carbonylation was shown in both patients' groups.
Conclusions: [^{11}C]-PK11195 Positron Emission Tomography imaging revealed neuroinflammation in dementia with Lewy bodies and Parkinson's disease, mirroring, even at a single subject level, the common and the different topographical distribution of neuropathological changes, yet in the earliest stages of the disease process. Focusing on those events that characterize parkinsonisms and Parkinson's disease may be the key to further advancing the understanding of pathogenesis and to taking these mechanisms forward as a means of defining targets for neuroprotection.

1. Introduction

Dementia with Lewy bodies (DLB) and Parkinson's disease (PD) are rather common neurodegenerative disorders both associated with neuronal loss and α-synuclein protein aggregated forms accumulation. As in many neurodegenerative disorders, the molecular mechanism accounting for neuronal loss and synapses damage is poorly understood. Oxidative damage, mitochondrial dysfunction and reactive microgliosis have been recently correlated to the pathogenesis and the progression of neuronal damage in PD, contributing to neuronal death [1–3].

Neuroinflammation occurs as a local response driven by microglia in absence of leukocyte infiltration, and may cause neuronal damage through cytotoxic molecules such as proinflammatory cytokines, proteinases, and reactive oxygen intermediates. Oxidative damage induces central nervous system protein modifications among which the carbonylation is the most common [4]. Its measurement aids to identify the rate of oxidative stress

* Corresponding author. Vita-Salute San Raffaele University, Nuclear Medicine Department and Division of Neuroscience, San Raffaele Scientific Institute, Via Olgettina 60, 20132 Milan, Italy. Tel.: +39 (0)2 26432224/2223; fax: +39 (0)2 26415202.
E-mail address: daniela.perani@hsr.it (D. Perani).

1353-8020/$ – see front matter © 2012 Published by Elsevier Ltd.
http://dx.doi.org/10.1016/j.parkreldis.2012.07.002

linked to the underlying neuropathology and has been suggested as a possible correlate of neuronal damage [4].

As for the anatomical correlates of neuroinflammation, post-mortem studies in PD patients reported activated microglia in the substantia nigra, putamen, cingulate cortex and medial temporal structures [5,6]. This suggests that the pathogenic insult induces an ongoing inflammatory/cytotoxic response, closely to sites of active brain pathology and at distance, possibly consequent to disconnection processes. An association between activated microglia and α-synuclein immunopositive neurons has been also reported in post-mortem DLB [7]. Thus, in these patients, the microglia-mediated inflammatory process seems to progressively surround degenerated neurons containing Lewy bodies inclusions.

Microglia may cause neuronal damage through the release of cytotoxic molecules, as supported by PD animal models [8]. During its activation, it expresses *de novo* the "peripheral benzodiazepine binding site" (PBBS), recently renamed translocator protein (TSPO) [9], a binding site which is abundant on cells of mononuclear phagocyte lineage, but usually poorly expressed in healthy brain.

The key role of neuroinflammation in neurological disorders has stimulated the search for specific radiotracers targeting the peripheral benzodiazepine receptor (PBR)/18 kDa translocator protein (TSPO), as hallmark of neuroinflammation.

PBR/TSPO has a very low level of expression in normal brain parenchyma and resident microglia of the healthy brain, while its expression is dramatically enhanced after activation of microglial cells following brain injury and neuroinflammation, as *in vivo* shown by [*N*methyl-11C](*R*)-1-(2-chlorophenyl)-*N*-(1-methylpropyl)-3-isoquinolinecarboxamide ([^{11}C]-PK11195) and Positron Emission Tomography (PET) imaging [1,10–12]. PK11195 is the prototype synthetic ligand widely used for the functional characterization of TPSO in view of the increased TSPO expression associated with activated microglia and infiltrating macrophages in states of disease [9]. Given this relative cellular selectivity, the measurement of TSPO dependent binding of PK11195, is considered a valid *in vivo* marker of the neuroinflammatory burden [1].

Consistent with experimental and post-mortem observations of a characteristically distributed pattern of microglia activation in areas of focal pathology, PBBS/TPSO expression significantly increases in patients with neurodegenerative processes. Regional increase of [^{11}C]-PK11195 PET binding has been indeed documented in patients with Alzheimer's disease closely to the pathological sites, thus in the entorhinal, temporoparietal and cingulate cortex [10] and in several neurological disorders (see as review [13]). Neuroinflammation has been also reported using [^{11}C]-PK11195 and PET in PD [14–16] and in parkinsonisms, such as corticobasal degeneration and progressive supranuclear palsy [17,18]. The previous *in vivo* PET studies of microglia activation in PD showed different patterns of inflammation involving either selectively midbrain and putamen [14,15] or more diffusely basal ganglia, pons and cortical regions [16].

No *in vivo* comparable studies are yet reported in DLB.

Our aim is thus to improve current knowledge on the possible role of neuroinflammation/cytotoxic environment associated with the pathologic changes of dopaminergic cells in DLB and to compare the results with comparably early PD.

DLB subjects, presenting with parkinsonism, but with a more diffuse neurodegeneration associated with dementia, might reveal a widespread brain pattern of neuroinflammation, also at a cortical level. We thus aim also at identifying putative specific PET patterns that could differentiate these diseases.

We also perform proteomic analysis of Cerebral Spinal Fluid (CSF) markers of oxidative stress in our patients, and comparing protein carbonylation levels with matched normal controls.

2. Material and methods

2.1. Subjects

We consecutively recruited drug-naïve early stage patients affected by either probable DLB (6 cases, 2 female and 4 male, mean age 72 ± 8.1) or probable idiopathic PD (6 cases, 3 female and 3 male, mean age 70.2 ± 2.9) according to the current diagnostic criteria [19,20] at the outpatient's clinic of the Neurologic Unit, Department of Neurological Sciences, San Raffaele Scientific Institute, Milan.

All patients were clinically evaluated by two expert neurologists and performed a thorough clinical-instrumental evaluation, including MRI, in order to disclose possible differential diagnosis (i.e. vascular parkinsonism). The standard MRI studies did not reveal region of focal atrophy in the patients.

In the PET study, patients were compared with a group of 11 gender-matched healthy volunteers (age range 29–60 years) previously recruited for different protocols. For the proteomic analysis, we collected CSF samples of 12 healthy age- and gender-matched individuals (5 female and 7 male, mean age 65 ± 9.4), who underwent lumbar puncture on account of a suspected neurological disease, which was excluded after a thorough CSF and clinico-instrumental evaluation. All controls reported negative history of neurologic disorders and were normal on neurological examination.

Demographic and clinical features of DLB and PD samples are summarized in Table 1. In particular, none of the PD patients presented cognitive decline or behavioral disorders, including hallucinations or sleep disorders, at a thorough neurobehavioral and neuropsychological evaluation. Global cognitive efficiency was within normal range (Mini Mental State Examination ≥27/30) for all PD subjects.

At the enrollment, all DLB and PD patients had a short disease duration (<1 years from symptoms onset), that was comparable in the two groups. Motor system impairment and disease severity were determined in both patients' groups by means of Unified Parkinson's Disease Rating Scale and Hoen and Yahr Stage. Our DLB patients showed more severe impairment at the motor UPDRS-III and Hoen and Yahr scales, consistent with reports in patients even in early phase [21].

A clinical-instrumental follow-up after 4-year from the clinical onset confirmed the diagnosis in all patients, which all presented a typical disease course.

Each subject gave written informed consent, following detailed explanation of the procedures, to take part in the study approved by the Local Ethical Committees, which included neurological evaluation, [^{11}C]-PK11195 PET imaging and CSF sample collection for CSF proteins carbonylation assay.

2.2. [^{11}C]-PK11195 PET imaging

2.2.1. Imaging protocol

All subjects underwent a [^{11}C]-PK11195 PET imaging, using a multi-ring PET tomograph (PET-CT system "Discovery STE" General Electric Medical Systems), installed at the Nuclear Department, San Raffaele Scientific Institute, Milan. Subjects

Table 1
Clinical and demographic features in probable Parkinson's disease (PD) and dementia of Lewy bodies (DLB).

	Mean/st. dev	PD1	PD2	PD3	PD4	PD5	PD6	Mean/st. dev	DLB1	DLB2	DLB3	DLB4	DLB5	DLB6
Patients														
Gender		M	F	F	M	M	F		F	F	M	M	M	M
Clinical subtype		Tremble	Akinetic	Tremble	Tremble	Tremble	Akinetic		–	–	–	–	–	–
Age at examination	70.2 ± 2.9	67	70	70	74	60	69	72 ± 8.1	82	65	72	62	77	73
Disease duration (months)	9.2 ± 1.9	7	8	12	9	10	10	10 ± 1.4	11	10	12	10	9	8
UPDRS I (cognitive functioning)	0.6 ± 0.8	0	2	1	0	0	0	6.2 ± 2.3	5	3	9	6	8	5
UPDRS II (activities of daily living)	4 ± 1	4	3	5	3	5	3	9 ± 1.5	11	10	9	8	7	5
UPDRS-III (motor examination)	7.2 ± 3.9	4	14	7	5	6	6	20 ± 4.6	21	22	26	17	14	12
Hoen and Yahr stage	1.5 ± 0.5	1	2	2	1	1.5	1	2.7 ± 0.27	3	2.5	3	2.5	2.5	2
MMSE (raw scores)	29 ± 1.41	30	28	27	30	30	29	24 ± 3.9	26	23	21	25	19	30

received an intravenous injection of approximately 370 MBq of [^{11}C]-PK11195 (mean dose 351 ± 74 MBq; range 244–481 MBq; radiochemical and chemical purity > 95%), prepared in our facility as previously described [22].

Thirty-five sequential scans (slice thickness 4.25 mm; axial field of view 15.5 cm) were simultaneously acquired in 3D mode up to 60 min from tracer injection. PET data were corrected for attenuation artefacts, radioactive decay and scatter. Transaxial images were reconstructed using a Shepp-Logan filter (cut-off 5 mm filter width) in the trans-axial plane, and a Shepp-Logan filter (cut-off 8.5 mm) in the axial direction. Each plane was realigned over time to correct for patient's movement during acquisition time using statistical parametric mapping (SPM99) software (http://www.fil.ion.ucl.ac.uk/spm/software).

2.2.2. Generation of parametric images

To obtain parametric images of the specific measure of the [^{11}C]-PK11195 binding, known as binding potential (BP), we use simplified reference tissue model (SRTM) [23]. This model allows the calculation of the BP and the relative influx of radioactivity using a brain area devoid of the neurochemical target of interest (the reference region) as input function. Since PBRs receptors are only minimally expressed in cortical normal brain parenchyma, it may be used as reference region for the calculation of the time course of the non-displaceable fraction of the radioligand. An operator independent analysis (cluster analysis) was used to define the input function since in pathological conditions is not possible to identify a priori a brain region devoid of activated microglia-linked PBRs. This analysis classify PET images in nine hierarchical clusters built according to their time–activity curves (TAC) shape and allows to extract regions where ligand kinetic approximate that of normal brain parenchyma [24]. Radioactivity distribution images were transformed voxel by voxel into binding potential images (BP) and relative influx images (RI) using the RPM (reversible reference tissue model) software developed by Gunn et al. [25].

The quantification of [^{11}C]-PK11195 PET imaging is intrinsically difficult, given the impossibility of defining "a priori" a brain region devoid of activated microglia-linked PBRs in the brain of patients with neurodegenerative disorders. We adopted a cluster analysis, as proposed in the literature and previously applied in PD patients [16,24], in order to extract regions where ligand kinetic approximate that of normal brain parenchyma, and limiting therefore the risk of including pathological tissue in the reference region. This approach, however, does not allow defining an anatomically consistent reference tissue between individuals across groups. The problems with [^{11}C]-PK11195 PET analysis are highlighted by the seeming disparity between the results reported by previous studies [14,16], and by the report of Bartels and coworkers [15], in which different analysis methods resulted in totally different results. This limitation, which cannot be overcome by the non-invasive quantification approaches currently available, should be taken into account when interpreting and comparing results of different groups.

2.2.3. Visual identification at single subject level

A threshold was defined as the mean plus two standard deviations of mean cortical BP of normal healthy subjects (mean + 2SD = 0.060 + 2*0.024 = 0.109) and thus applied to patients parametric images. This approach was previously reported for [^{11}C]-PK11195 BP images of patients to enhance cortical signal, thus providing a better visualization of microglia activation at single subject level [24].

2.2.4. Regions of Interest definition

A Regions of Interest (ROIs) analysis was used to better identify the regional distribution of the [^{11}C]-PK11195 BP. RI parametric images deriving from RPM software, were normalized to the Montreal Neurological Institute (MNI) stereotactic space using the SPM [^{18}F]FDG PET template and the transformation parameters obtained during the normalization and co-registration procedures applied to BP images. A set of Region of Interest (ROIs) was chosen (see list in Fig. 1 and Table 2), based on the main pathologically cortical and subcortical structures involved in PD and DLB. The ROIs were bilaterally positioned on normalized BP images of each single subject on the basis of SPM MRI template.

2.2.5. Regions of Interest analysis

Statistical analyses of [^{11}C]-PK11195 BP values derived from ROI analysis were carried out with SPSS 16 for Windows, SPSS Inc., Chicago, Illinois.

Differences between groups were assessed using ANCOVA and Tukey's HSD post hoc test ($p < 0.001$ uncorrected). For post hoc analysis, we choose also a more lenient threshold ($p < 0.01$) in order to explore more subtle effects. Being aware of the age difference between controls and patients, we considered age as a potential confounding variable and included it in the analysis as nuisance variable. Nevertheless, it has to be considered that the previous studies [14,26,27] investigating the effect of age on [^{11}C]-PK11195 BP, revealed a consistent age dependent increase only in the thalamus and midbrain. None showed effects in the basal ganglia and substantia nigra, regions highly related to parkinsonism, and specifically investigated in our study. Thus, we expected in both patients' groups a disease specificity to be detected by region analysis with large and significant differences with respect to normal controls.

We also show the value of [^{11}C]-PK11195 BP in each individual patient for all the included brain regions compared with mean and 2SD in healthy controls (see Table 2).

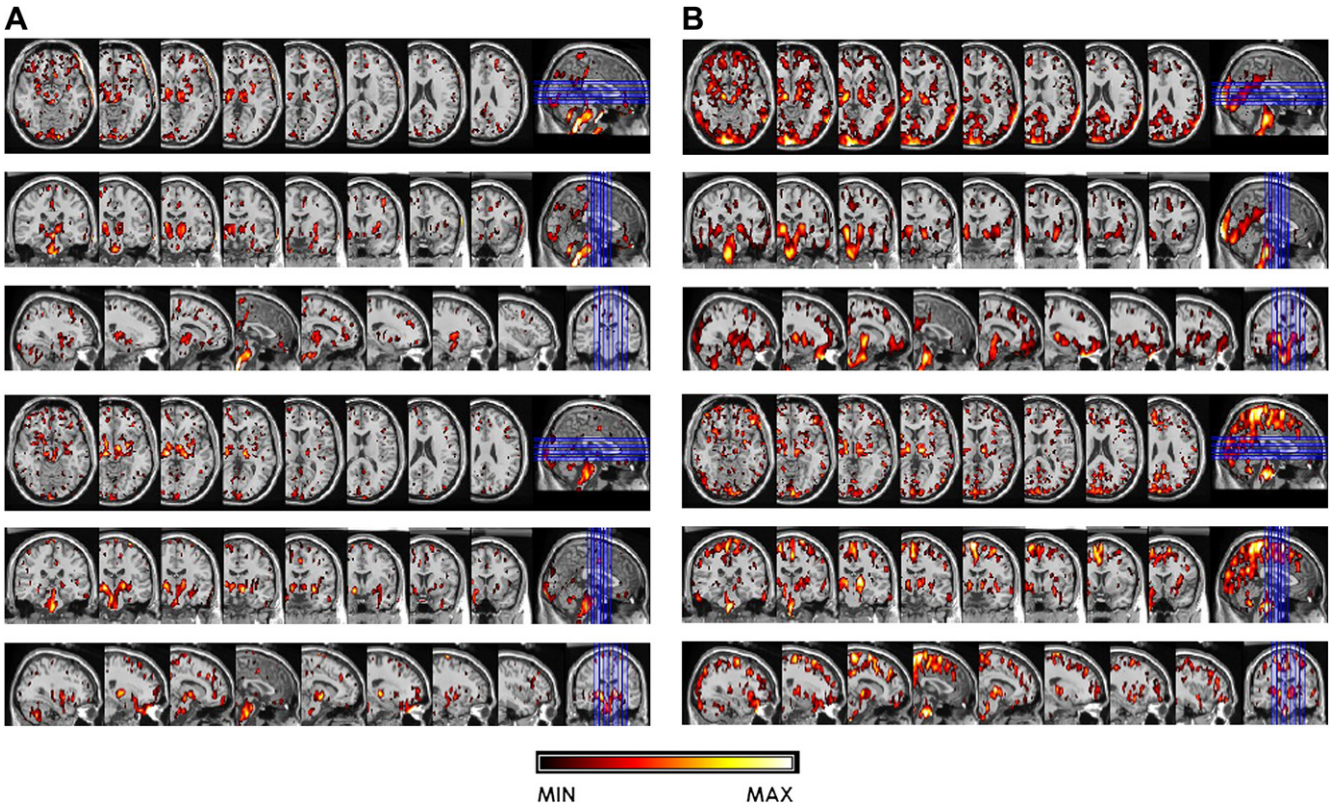

Fig. 1. Single subject [^{11}C]-PK11195 uptake in two Parkinson's disease (PD) (A) and dementia with Lewy bodies (DLB) (B) cases. Note the comparable subcortical involvement in the PD (PD2 and PD4) and DLB (DLB1 and DLB5) cases and the widespread microglia activation at the cortical level in DLB (see text for details).

Table 2
ROIs [^{11}C]-PK11195 binding potential (BP) mean values, SD and mean BP + 2SD values (in bold) for the group of healthy controls (CTR), and individual ROIs [^{11}C]-PK11195 BP values, and mean BP and SD values for dementia with Lewy bodies (DLB) and Parkinson's disease (PD) groups. In bold, mean BP values of DLB and PD groups overcoming mean BP + 2 SD values of CTR group.

Regions of Interest (ROIs)	FLC	PLC	TLC	TP	PrC	OMC	OLC	Ant CING	Post CING	CBL	HIPP	AMYG	CAU	PUT	THAL	SN
CTR																
Mean	0.06	0.06	0.06	0.04	0.06	0.08	0.08	0.06	0.07	0.12	0.11	0.12	0.08	0.12	0.29	0.23
SD	0.02	0.03	0.01	0.01	0.02	0.03	0.02	0.02	0.02	0.04	0.04	0.05	0.03	0.03	0.04	0.07
Mean + 2SD	**0.10**	**0.12**	**0.09**	**0.07**	**0.10**	**0.14**	**0.13**	**0.11**	**0.11**	**0.20**	**0.18**	**0.23**	**0.13**	**0.18**	**0.38**	**0.36**
DLB																
1	0.36	0.23	0.29	0.34	0.27	0.30	0.26	0.36	0.30	0.27	0.32	0.25	0.34	0.36	0.58	0.67
2	0.13	0.23	0.24	0.24	0.20	0.24	0.21	0.15	0.21	0.28	0.26	0.30	0.09	0.21	0.43	0.59
3	0.15	0.04	0.06	0.11	0.05	0.03	0.04	0.09	0.09	0.16	0.04	0.06	0.22	0.15	0.31	0.33
4	0.15	0.20	0.17	0.10	0.25	0.12	0.21	0.25	0.14	0.19	0.03	0.07	0.12	0.19	0.38	0.48
5	0.22	0.16	0.21	0.26	0.22	0.21	0.23	0.23	0.28	0.26	0.23	0.29	0.32	0.30	0.41	0.37
6	0.06	0.07	0.05	0.07	0.13	0.15	0.12	0.02	0.10	0.13	0.06	0.11	0.05	0.16	0.30	0.34
Mean	**0.18**	**0.16**	**0.17**	**0.18**	**0.19**	**0.18**	**0.18**	**0.18**	**0.19**	**0.21**	0.16	0.18	**0.19**	**0.23**	**0.40**	**0.46**
SD	0.10	0.08	0.10	0.11	0.08	0.10	0.08	0.12	0.09	0.06	0.13	0.11	0.12	0.08	0.10	0.14
PD																
1	0.11	0.10	0.10	0.17	0.13	0.10	0.16	0.14	0.11	0.24	0.13	0.28	0.16	0.25	0.33	0.41
2	0.09	0.06	0.07	0.10	0.07	0.09	0.10	0.13	0.14	0.25	0.14	0.17	0.19	0.21	0.39	0.33
3	0.13	0.12	0.20	0.15	0.16	0.12	0.17	0.14	0.17	0.14	0.11	0.17	0.14	0.18	0.35	0.42
4	0.12	0.14	0.13	0.14	0.10	0.14	0.27	0.15	0.06	0.14	0.17	0.21	0.18	0.21	0.40	0.41
5	0.17	0.19	0.16	0.10	0.16	0.09	0.13	0.20	0.15	0.11	0.26	0.25	0.23	0.30	0.39	0.56
6	0.11	0.07	0.11	0.06	0.10	0.16	0.13	0.11	0.14	0.14	0.10	0.09	0.10	0.17	0.34	0.57
Mean	**0.12**	0.11	**0.13**	**0.12**	**0.12**	0.12	**0.16**	**0.14**	**0.13**	0.17	0.15	0.19	**0.17**	**0.22**	0.37	**0.45**
SD	0.03	0.05	0.05	0.04	0.04	0.03	0.06	0.03	0.04	0.06	0.06	0.07	0.05	0.05	0.03	0.09

FLC, frontal lateral cortex; PLC, parietal lateral cortex; TLC, temporal lateral cortex; TP, temporal pole; PrC, precuneus; OMC, occipital medial cortex; OLC, occipital lateral cortex; Ant CING and Post CING, anterior and posterior cingulate cortices; CBL, cerebellum; HIPP, hippocampus; AMYG, amygdale; CAU, caudate; PUT, putamen; THAL, thalamus; SN, substantia nigra.

2.3. CSF proteins carbonylation assay

CSF samples (0.8–1 mL) were collected in 2 mL plastic transfer tubes by means of lumbar puncture. The analyzed samples were from 5 PD patients (PD1; PD2; PD3; PD4; PD5 cases described in Table 1), all 6 DLB patients and 12 healthy controls (HC). Immediately after collection, the CSF samples were transferred in 1,5 mL polypropylene tubes (Eppendorf, Milan, IT) and centrifuged (1100 rpm, 8 min at 4 °C) to eliminate cells. Then, protein concentrations were determined by the Bradford method. The samples were immediately processed in order to avoid artifactual environmental oxidation. The eventual red blood cells contamination of CSF was evaluated by hemoglobin detection measured by WB with specific antibodies (Santa Cruz SC31110, CA). PD3 sample resulted positive, so excluded by the carbonylation analysis.

Carbonylation analysis was thus performed in 10 patients (4 PD and 6 DLB) by means of the OxyBlot Protein Oxidation Detection Kit (Chemicon, USA) on the basis of carbonyl group derivatization with 2,4-dinitrophenilhydrazine (DNPH) performed on 100 μg of total CSF proteins as described by manufacturer's instructions.

After derivatization, proteins were resolved by 12% acrylamide SDS-PAGE and electro-transferred onto nitrocellulose membranes as previously described [28]; carbonyl groups were detected by Western blot (WB) performed with an anti-DNPH antibody, as in Oliveri et al. [29]. Images were acquired by means of a laser densitometer (Molecular Dynamics, Sunnyvale, CA), and evaluation of relative abundance of carbonylation consisted in the analysis of optical density (OD) by means of Progenesis PG240 software (Nonlinear dynamics, Newcastle, UK) normalized on the Ponceau staining as loading control [30].

Statistical analysis of protein carbonylation levels was done by Mann–Whitney test since the data not passed the normality test for Gaussian distribution; two-tailed p value was used for the comparison of two means and standard error.

3. Results

3.1. [^{11}C]-PK11195 PET imaging

Healthy subjects presented [^{11}C]-PK11195 BP values comparable to those previously reported in literature [10,16,26]: the lowest in cortical ROIs (mean 0.06 ± 0.01) and in the striatum (mean 0.10 ± 0.02), and the highest in the thalamus (mean 0.29 ± 0.04) and pons (mean 0.34 ± 0.06). In our control sample, Spearman correlation analysis failed to show any significant correlation between age and [^{11}C]-PK11195 binding in all the selected regions. A trend toward an increase in tracer binding was present in our sample and limited to the thalamus, thus consistent with previous studies [14,26,27].

3.1.1. Visual identification at single subject level

The visual inspection of the [^{11}C]-PK11195 BP images in single subjects showed increased microglia activation in putamen and substantia nigra in all DLB and PD patients. DLB patients showed also increased [^{11}C]-PK11195 BP in the caudate, and an extended microglial activation in several cortical regions, heterogeneously distributed among patients. In few PD cases BP increases were present also at the anterior cingulate and medial prefrontal regions (see Fig. 1A and B as examples).

3.1.2. Regions of Interest analysis

ANCOVA showed a significant ($p < 0.001$) group level effect on [^{11}C]-PK11195 BP, thus revealing the differences in PD and DLB patients compared to normal controls. Post Hoc comparisons showed in DLB patients significant BP increases both in subcortical (basal ganglia, substantia nigra) and cortical regions, involving several associative areas, as well as the cerebellum, whereas in the PD group, a more limited pattern of microglia activation, affecting only the putamen and substantia nigra was present (see Fig. 2).

As shown in Table 2 individual patients' BP differed from controls, overcoming in several regions the 2SD.

3.2. Analysis of CSF proteins carbonylation

Analysis of total protein carbonylation in the CSF from both DLB and PD patients showed significantly greater levels compared to controls ($p = 0.0044$ PD *vs.* controls and $p = 0.017$ DLB *vs.* controls, respectively by Mann–Whitney test; PD: $n = 4$, OD 132.31 ± 23.22 SEM; DLB: $n = 6$, OD 96.91 ± 17.02 SEM; controls: $n = 12$, 48.96 ± 5.96 SEM). No statistical difference was observed between DLB and PD groups ($p = 0.2571$). These results demonstrated that CSF proteins undergo oxidative modifications even at an early stage of the pathological events in both disorders.

4. Discussion

This study reports for the first time the activation of microglial cells in DLB assessing *in vivo* the amount and the anatomical

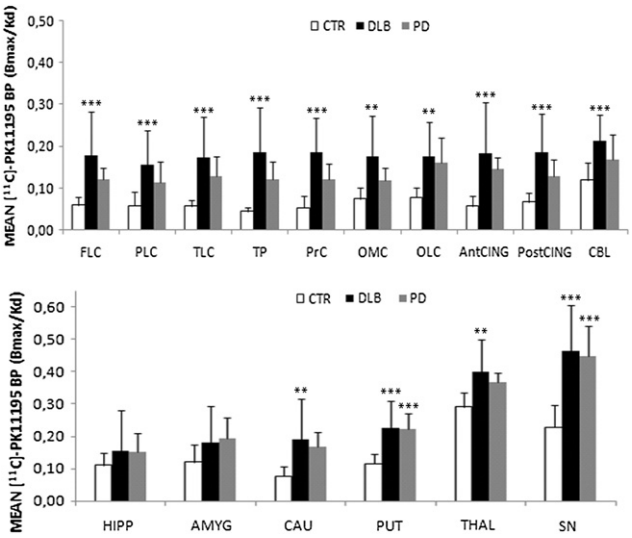

Fig. 2. Bar graph of regional [^{11}C]-PK11195 binding potential (BP) in healthy controls (CTR), and dementia with Lewy bodies (DLB) and Parkinson's disease (PD) patients. Asterisks indicate statistically significant differences between DLB and PD patients, respectively, *versus* CTR on Tukey's post hoc test. Statistic threshold: $^{**}p < 0.01$, $^{***}p < 0.001$. FLC, frontal lateral cortex; PLC, parietal lateral cortex; TLC, temporal lateral cortex; TP, temporal pole; PrC, precuneus; OMC, occipital medial cortex; OLC, occipital lateral cortex; Ant CING and post CING, anterior and posterior cingulate cortices; CBL, cerebellum; HIPP, hippocampus; AMYG, amygdale; CAU, caudate; PUT, putamen; THAL, thalamus; SN, substantia nigra.

distribution of neuroinflammatory response in a very early disease phase. It provides new evidence for an active role of microglia in DLB at the nigro-striatal pathway and at cortical level [7], suggesting a specific pattern of topographical distribution of [^{11}C]-PK11195 BP. It well corresponds to the deposition of Lewy bodies which involves the whole brain cortex, and in particular frontal and temporal regions. According to the three neuropathological phenotypes (brainstem, transitional/limbic, and diffuse neocortical) [19], neuroinflammatory changes may thus occur at several cortical regions in DLB. The presence of microglia activation in the substantia nigra and putamen was comparable to that found in the PD patient group, whose inflammatory pattern confirmed previous PET findings [14–16] in agreement with the neuropathological distribution of microglia activation, which mostly involves the pars compacta of the substantia nigra, close to the site of dopaminergic neurons degeneration [5].

We confirmed an increased BP in PD patients also in the putamen, whose neuroinflammatory changes are probably due to neurodegeneration of nigral dopaminergic projections [16,31]. Possibly, changes in microglial activation are likely to occur in parallel with loss of dopaminergic terminals, as further demonstrated in some PD cases in this series, in which we found microglia activation also in the anterior cingulate cortex and prefrontal regions (see Table 2 and Fig. 2). According to Braak's stages [32], neuropathological changes in PD occur firstly in substantia nigra and brainstem in general, and later in basal ganglia and cingulate cortex or associative cortical areas. Considering the anatomical correspondence between neuropathological changes and *in vivo* PET microglia activation, neuroinflammation in PD may be an early but chronic process that intensifies during progressive neurodegeneration, as also suggested by a previous study reporting higher BP values in advanced PD patients compared to *de novo* PD [15]. Thus, while neurodegeneration in PD specifically induces selective cell loss in the substantia nigra and damage to the nigro-striatal pathways, with a secondary involvement of subcortical and cortical structures [6], the neuropathological hallmarks in DLB are more diffuse up to the associative cerebral cortex, since the beginning [19]. Besides, microglial activation in DLB, might be also associated and influenced by amyloid plaques formation [33].

The different and significant group-effects in the neuroinflammatory patterns were also evident at the single subject level (see Fig. 1).

Although a pilot study, our results highly suggest that [^{11}C]-PK11195 PET imaging represents a neuroanatomical indicator of neuroinflammation even in early disease phase. Moreover, this PET study provides individual relevant information on pattern location and spreading of neuroinflammation. Noteworthy, microglia activation was present in the very early disease phase (all patients were within 1 year from the clinical onset), possibly reflecting a change from a healthy brain to the beginning of the pathological process. Though microglia activation is not a disease specific marker, as the region analysis documented, it provides important topographical information that revealed consistency and differences in the two patient groups.

Furthermore, both DLB and PD patients showed comparable high levels of carbonylated proteins reflecting unspecific CSF oxidative sufferance and changes in the environment surrounding the degenerating brain tissue, as reported in other neurodegenerative conditions [27]. This might reflect accelerated protein aging, likely induced by oxidative pathological processes [34,35]. Post-mortem study in PD patients documented indeed alterations occurring in a range of cytokines both in the nigro-striatal system and in the CSF [6].

Overall, despite the limitation of the study, mostly concerning sample-size and quantification of [^{11}C]-PK11195 PET imaging, these *in vivo* findings in DLB and PD subjects with a 4-year clinical follow-up confirmed diagnosis and typical disease course, support specific neuroinflammatory signatures that might be helpful in monitoring future interventional trials, even at a single subject level, and in the early phase of the disease. Nevertheless, longitudinal studies are needed to evaluate the association of biomarker evidence for microglial activation with clinical disease progression to better clarify the harmful or protective role of microglial activation in neurodegenerative disorders.

Disclosure of interest

None of the authors report any disclosures.

Acknowledgments

We acknowledge Dr. Alessandra Marcone for having provided two DBL subjects and Mario Matarrese for [^{11}C]-PK11195 delivery. The study was supported by the DIMI LSHB-CT-2005-512146. MA was supported by Fondazione CARIPLO (Nobel-Guard project) and by MoH, RF07-ALS.

References

[1] Bartels AL, Leenders KL. Neuroinflammation in the pathophysiology of Parkinson's disease: evidence from animal models to human *in vivo* studies with [^{11}C]-PK11195 PET. Mov Disord 2007 Oct 15;22(13):1852–6.
[2] Schapira AH, Jenner P. Etiology and pathogenesis of Parkinson's disease. Mov Disord 2011 May;26(6):1049–55.
[3] Dawson TM, Dawson VL. Molecular pathways of neurodegeneration in Parkinson's disease. Science 2003 Oct 31;302(5646):819–22.
[4] Dalle-Donne I, Giustarini D, Colombo R, Rossi R, Milzani A. Protein carbonylation in human diseases. Trends Mol Med 2003 Apr;9(4):169–76.
[5] McGeer PL, Itagaki S, Boyes BE, McGeer EG. Reactive microglia are positive for HLA-DR in the substantia nigra of Parkinson's and Alzheimer's disease brains. Neurology 1988 Aug;38(8):1285–91.
[6] Imamura K, Hishikawa N, Sawada M, Nagatsu T, Yoshida M, Hashizume Y. Distribution of major histocompatibility complex class II-positive microglia

and cytokine profile of Parkinson's disease brains. Acta Neuropathol 2003 Dec; 106(6):518–26 [Epub 2003 Sep. 25].
[7] Mrak RE, Griffin WS. Common inflammatory mechanisms in Lewy body disease and Alzheimer disease. J Neuropathol Exp Neurol 2007 Aug;66(8): 683–6.
[8] Teismann P, Tieu K, Choi DK, Wu DC, Naini A, Hunot S, et al. Cyclooxygenase-2 is instrumental in Parkinson's disease neurodegeneration. Proc Natl Acad Sci U S A 2003 Apr 29;100(9):5473–8 [Epub 2003 Apr 17].
[9] Papadopoulos V, Baraldi M, Guilarte TR, Knudsen TB, Lacapère J-J, Lindemann P, et al. Translocator protein (18 kDa): new nomenclature for the peripheral-type benzodiazepine receptor based on its structure and molecular function. Trends Pharmacol Sci 2006 Aug;27(8):402–9.
[10] Cagnin A, Brooks DJ, Kennedy AM, Gunn RN, Myers R, Turkheimer FE, et al. *In-vivo* measurement of activated microglia in dementia. Lancet 2001 Aug 11; 358(9280):461–7.
[11] Chauveau F, Boutin H, Van Camp N, Dollé F, Tavitian B. Nuclear imaging of neuroinflammation: a comprehensive review of [^{11}C]-PK11195 challengers. Eur J Nucl Med Mol Imaging 2008;35(12):2304–19 [Epub 2008 Oct 1].
[12] Turkheimer FE, Edison P, Pavese N, Roncaroli F, Anderson AN, Hammers A, et al. Reference and target region modelling of [^{11}C]-(R)-PK11195 brain studies. J Nucl Med 2007;48(1):158–67.
[13] Cagnin A, Kassiou M, Meikle SR, Banati RB. Positron emission tomography imaging of neuroinflammation. Neurotherapeutics 2007 Jul;4(3):443–52.
[14] Ouchi Y, Yoshikawa E, Sekine Y, Futatsubashi M, Kanno T, Ogusu T, et al. Microglial activation and dopamine terminal loss in early Parkinson's disease. Ann Neurol 2005 Feb;57(2):168–75.
[15] Bartels AL, Willemsen AT, Doorduin J, de Vries EF, Dierckx RA, Leenders KL. [^{11}C]-PK11195 PET: quantification of neuroinflammation and a monitor of anti-inflammatory treatment in Parkinson's disease? Parkinsonism Relat Disord 2010 Jan;16(1):57–9 [Epub 2009 May 31].
[16] Gerhard A, Pavese N, Hotton G, Turkheimer F, Es M, Hammers A, et al. *In vivo* imaging of microglial activation with [^{11}C](R)-PK11195 PET in idiopathic Parkinson's disease. Neurobiol Dis 2006 Feb;21(2):404–12 [Epub 2005 Sep. 21].
[17] Gerhard A, Watts J, Trender-Gerhard I, Turkheimer F, Banati RB, Bhatia K, et al. *In vivo* imaging of microglial activation with [^{11}C](R)-PK11195 PET in corticobasal degeneration. Mov Disord 2004 Oct;19(10):1221–6.
[18] Gerhard A, Trender-Gerhard I, Turkheimer F, Quinn NP, Bhatia KP, Brooks DJ. *In vivo* imaging of microglial activation with [^{11}C](R)-PK11195 PET in progressive supranuclear palsy. Mov Disord 2006 Jan;21(1):89–93.
[19] McKeith IG, Dickson DW, Lowe J, Emre M, O'Brien JT, Feldman H, et al. Diagnosis and management of dementia with Lewy bodies: third report of the DLB consortium. Neurology 2005 Dec 27;65(12):1863–72 [Epub 2005 Oct 19].
[20] Gelb DJ, Oliver E, Gilman S. Diagnostic criteria for Parkinson disease. Arch Neurol 1999 Jan;56(1):33–9.
[21] Müller J, Wenning GK, Jellinger K, McKee A, Poewe W, Litvan I. Progression of Hoehn and Yahr stages in Parkinsonian disorders: a clinicopathologic study. Neurology 2000 Sep 26;55(6):888–91.
[22] Matarrese M, Moresco RM, Cappelli A, Anzini M, Vomero S, Simonelli P, et al. Labeling and evaluation of N-[^{11}C]methylated quinoline-2-carboxamides as potential radioligands for visualization of peripheral benzodiazepine receptors. J Med Chem 2001 Feb 15;44(4):579–85.
[23] Lammertsma AA, Hume SP. Simplified reference tissue model for PET receptor studies. Neuroimage 1996 Dec;4(3 Pt 1):153–8.
[24] Banati RB, Newcombe J, Gunn RN, Cagnin A, Turkheimer F, Heppner F, et al. The peripheral benzodiazepine binding site in the brain in multiple sclerosis: quantitative *in vivo* imaging of microglia as a measure of disease activity. Brain 2000 Nov;123(Pt 11):2321–37.
[25] Gunn RN, Lammertsma AA, Hume SP, Cunningham VJ. Parametric imaging of ligand-receptor binding in PET using a simplified reference region model. Neuroimage 1997 Nov;6(4):279–87.
[26] Debruyne JC, Van Laere KJ, Versijpt J, De Vos F, Eng JK, Strijckmans K, et al. Semiquantification of the peripheraltype benzodiazepine ligand [^{11}C]-PK11195 in normal human brain and application in multiple sclerosis patients. Acta Neurol Belg 2002 Sep;102(3):127–35.
[27] Schuitemaker A, van der Doef TF, Boellaard R, Van der Flier WM, Yaqub M, Windhorst AD, et al. Microglial activation in healthy aging. Neurobiol Aging 2012 Jun;33(6):1067–72 [Epub 2010 Nov 3].
[28] Conti A, Iannaccone S, Sferrazza B, De Monte L, Cappa S, Franciotta D, et al. Differential expression of ceruloplasmin isoforms in the cerebrospinal fluid of amyotrophic lateral sclerosis patients. Proteomics Clin Appl 2008 Dec;2(12):1628–37 [Epub 2008 Oct 7].
[29] Olivieri S, Conti A, Iannaccone S, Cannistraci CV, Campanella A, Barbariga M, et al. Ceruloplasmin oxidation, a feature of Parkinson's disease CSF, inhibits ferroxidase activity and promotes cellular iron retention. J Neurosci 2011 Dec 14;31(50):18568–77.
[30] Romero-Calvo I, Ocón B, Martínez-Moya P, Suárez MD, Zarzuelo A, Martínez-Augustin O, et al. Reversible Ponceau staining as a loading control alternative to actin in Western blots. Anal Biochem 2010;401(2):318–20.
[31] Cagnin A, Myers R, Gunn RN, Lawrence AD, Stevens T, Kreutzberg GW, et al. *In vivo* visualization of activated glia by [^{11}C](R)-PK11195-PET following herpes encephalitis reveals projected neuronal damage beyond the primary focal lesion. Brain 2001 Oct;124(Pt 10):2014–27.
[32] Braak H, Del Tredici K, Rüb U, de Vos RA, Jansen Steur EN, Braak E. Staging of brain pathology related to sporadic Parkinson's disease. Neurobiol Aging 2003 Mar-Apr;24(2):197–211.
[33] Maetzler W, Liepelt I, Reimold M, Reischl G, Solbach C, Becker C, et al. Cortical PIB binding in Lewy body disease is associated with Alzheimer-like characteristics. Neurobiol Dis 2009 Apr;34(1):107–12. 2008.
[34] Grimm S, Hoehn A, Davies KJ, Grune T. Protein oxidative modifications in the ageing brain: consequence for the onset of neurodegenerative disease. Free Radic Res 2011 Jan;45(1):73–88 [Epub 2010 Sep. 6].
[35] Glass CK, Saijo K, Winner B, Marchetto MC, Gage FH. Mechanisms underlying inflammation in neurodegeneration. Cell 2010 Mar 19;140(6): 918–34.